Published in final edited form as:
J Phys Chem B. 2009 October 1; 113(39): 13079–13085. doi:10.1021/jp905001q.

Translational and rotational dynamics of monosaccharide solutions

Gérald Lelong[a,†,*], **W. Spencer Howells**[b], **John W. Brady**[d], **César Talon**[d], **David L. Price**[e], and **Marie-Louise Saboungi**[a]

[a] Centre de Recherche sur la Matière Divisée, Université d'Orléans / CNRS-UMR 6619, 45071 Orléans, France

[b] Rutherford-Appleton Laboratory, Chilton, Oxon OX11 0QX, United Kingdom

[d] Department of Food Sciences, Cornell University, Ithaca, NY 14853, USA

[e] Conditions Extrêmes et Matériaux : Haute Température et Irradiation, CNRS-UPR 3079, 45071 Orléans, France

Abstract

Molecular dynamics computer simulations have been carried out on aqueous solutions of glucose at concentrations bracketing those previously measured with quasi-elastic neutron scattering (QENS), in order to investigate the motions and interactions of the sugar and water molecules. In addition, QENS measurements have been carried out on fructose solutions to determine whether the effects previously observed for glucose apply to monosaccharide solutions. The simulations indicate a dynamical analog between higher solute concentration and lower temperature that could provide a key explanation of the bioprotective phenomena observed in many living organisms. The experimental results on fructose solutions show qualitatively similar behavior to the glucose solutions. The dynamics of the water molecules are essentially the same, while the translational diffusion of the sugar molecules is slightly faster in the fructose solutions.

Keywords

monosaccharide; water; dynamics; neutron scattering; molecular dynamics

I. Introduction

Osmotic dehydration is a well-known process based on the immersion of fresh products such as fruits into a concentrated sugar or salt solutions.[1,2] The osmotic pressure difference between the fruit and the solution leads to partial removal of water from the plant tissues and migration of the osmotic solutes back into the fruit. Among currently used osmotic media, solutions of the monosaccharides glucose and fructose are particularly efficient in water replacement and preservation of fruit structures. In a similar mechanism, many living organisms use mono- and disaccharides, either produced internally or accumulated in their tissues, to protect themselves against severe climates.[3,4,5,6,7] These examples illustrate the important role that hydrated sugars play in biological processes.

* Corresponding author: gerald.lelong@impmc.jussieu.fr.
†Present Address: Institut de Minéralogie et Physique des Milieux Condensés, Université Paris 6 / Université Paris 7 / CNRS-UMR 7590 / IPGP, 75015 Paris, France.

Carbohydrates have complicated structures, including overlapping polar and apolar groups, inter- and intramolecular hydrogen bonds, and a large number of hydroxyl groups, conferring a strong hydrophilic character. Thus, sugars exhibit a natural affinity for water, as shown by their high solubility. The collective structure of bulk water is even more complex, with its well-organized hydrogen bonded network and long list of unusual properties.[8,9] Depending on their configurations and conformations, the structuring imposed on water by sugars can be more or less compatible with the hydrogen bond network of bulk water, in some cases leading to disruption of that network or changes in the sugar conformation due to the surrounding water molecules.[10,11] The stereochemistry of sugars affects the physico-chemical properties of their solutions, as shown by the significant variations in density, glass transition temperature (T_g), viscosity and hydration number.[12] The two hexoses - glucose and fructose - are particularly interesting because they constitute the most prominent monosaccharides occurring in living organisms. While glucose is an aldose, and fructose a ketose, it remains that their topologies are quite different. At equilibrium at room temperature, for example, glucose consists of a mixture of two six-membered ring forms α-D-glucopyranose (38%) and β-D-glucopyranose (62%), while fructose exhibits four topological configurations of its five- and six-membered rings: α-D-fructopyranose (2.3%), β-D-fructopyranose (72%), α-D-fructofuranose (5.2%) and β-D-fructofuranose (20%) (Fig. 1).[13,14] These different morphologies lead to significant variations in the properties of their solutions such as density (1.1209 $g.cm^{-3}$ for glucose *vs.* 1.1251 for fructose at 30 wt.%)[12], solubility (0.08029 for glucose[15] *vs.* 0.3750 for fructose[16]), and viscosity (3.46 mPa.s for glucose *vs.* 3.07 for fructose at 30 wt.%).[17] It is therefore important to study the effects of stereochemistry on the dynamical properties of the aqueous solutions of these two monosaccharides.

Recently, we reported quasielastic neutron scattering (QENS) measurements of the dynamics of both water and glucose molecules in dilute and concentrated solutions.[18,19] A diffusive process with a relaxation time τ gave rise to a peak in the scattering function $S(Q,E)$ centered at zero energy transfer E with a full width at half-maximum (FWHM) ΔE related to $1/\tau$. In the simple case of a purely exponential relaxation, $S(Q,E)$ has a Lorentzian shape with $\Delta E = 2\hbar l^2 Q^2/6\tau$, where l is a characteristic jump distance and Q is the scattering vector. Thus, QENS measurements carried out as a function of both E and Q give temporal and spatial information about the diffusive process. The relaxation time τ_R for rotational diffusion can also be extracted.

Recently, we found that the addition of glucose to the water caused a substantial slowing, by a factor of 10 for the translational diffusion and 3-4 for the rotational motion at the highest concentration studied, 1:11 $C_6H_{12}O_6$:H_2O.[18] The glucose translational diffusion and the rotational motions slowed down considerably with a decrease in concentration: for example, the diffusion coefficient dropped by a factor of 5 in going from a 1:55 to a 1:11 concentration.[19] More recently, we have studied the effects of confinement in silica gel on the dynamics of glucose and trehalose solutions.[20,21]

The present work has two objectives. First, numerical molecular dynamics (MD) simulations were carried out on glucose solutions, at concentrations bracketing those measured by QENS in order to investigate in detail the processes involved and to compare them with experiments. Secondly, the dynamics of aqueous solutions of fructose were measured by QENS to check the universality of the behavior observed in glucose solutions. Thus, we can obtain an insight into the role of the stereochemistry on the global dynamics.

II. Experimental

A. MD Computer Simulations

Classical MD simulations were carried out for glucose:H_2O solutions with 1, 3 and 5 molal concentrations, respectively. These three simulations span the concentration range of the QENS

measurements reported previously.[18,19] The total numbers of the glucose anomers were chosen to be as close as possible to the tautomeric equilibrium values, with 36 α-glucose and 64 β-glucose molecules, and the box size was selected to match the experimental densities at the desired temperature. The simulation parameters are listed in Table 1. The water molecules were represented with the SPC/E model[22] and the CSFF force field was employed for the glucose.[23] Because quantitative estimates of the diffusional behavior were sought, all simulations were performed as microcanonical ensembles with the CHARMM program,[24] using a time step of 1 fs and with the chemical bonds to the hydrogen atoms kept fixed with the SHAKE program.[25] The van der Waals and electrostatic interactions were smoothly truncated on a neutral group basis using switching functions from 13 to 15 Å. The initial temperature of each glucose solution was set at a temperature of approximately 100 K by random selection of each of the Cartesian components of the velocity of each atom from a Maxwell-Boltzmann distribution, subject to the geometric constraints imposed by the SHAKE algorithm. All solutions were heated at the rate of 20 K/ps until they reached the desired simulation temperatures, 240, 260, 280, 300, 320 and 340 K, respectively. The simulations were then equilibrated for a period of 50 ps, during which time the velocities were periodically rescaled if the average temperature of the system deviated from the target temperature by more than ±3.0 K. This equilibration was then followed by an additional 2 ns trajectory without scaling which was used for analysis. The actual system temperature and total energy were monitored during this data collection period to assure temperature stability and energy conservation.

B. Samples

Selective hydrogen:deuterium isotope substitution is a valuable tool for sorting out the dynamics of a complex organic system with neutron scattering. Since the total bound-atom cross section for H (81.7 b) is much larger than that of D (7.6 b) and most other elements, the measured intensity is dominated by the scattering from the H atoms. Thus, the water dynamics can be highlighted by measuring samples with deuterated sugar dissolved in H_2O,[18] and the sugar dynamics with samples with isotopically-natural sugar dissolved in D_2O.[19] Unfortunately, the experimental situation is complicated by the unavoidable exchange of 5 of the 12 hydrogen atoms of the glucose molecule by hydrogen from the solvent water so that, in the first of the two cases just described, some contribution to the scattering from the sugar molecules is inevitable. The problem is alleviated to some extent by the fact that the time scale of the solvent dynamics is about 5 times that of the solute dynamics.

In order to disentangle the dynamics of the solvent from that of the solute, three samples were prepared with the following characteristics (Table 2): (1) Pure H_2O, as a reference point, (2) a solution of 7d-fructose (Sigma Aldrich, D-fructose, $C_6H_5D_7O_6$, deuterated at the C_1, C_2, C_3, C_4, C_5 and twice at the C_6 position) in H_2O at a molar concentrations of 1:24.5 $C_6H_5D_7O_6$:H_2O, corresponding to a concentration of 2.3 molal, or 29 wt.%, in a fully protonated solution, and (3) a solution of deuterated fructose in D_2O at the same molar concentration. In the case of the sample 2, D-fructose was mixed with heavy water, dried and re-mixed with D_2O to avoid deuteration of the water by exchangeable hydrogens.

C. QENS Experiments

The QENS experiments on the fructose solutions were carried out on the IRIS Backscattering Spectrometer[26] at the ISIS pulsed spallation source at the Rutherford-Appleton Laboratory, Chilton, UK, at an incident wavelength of 6.7 Å. The samples were loaded into aluminum annular cans with an annular distance of 0.5 mm (0.1 mm in the case of the H_2O and d-fruc +H_2O samples) and placed within the radiation shield of a closed-cycle refrigerator, in which the temperature could be controlled to ±1 K. The *Q* range was 0.46-1.84 $Å^{-1}$ and runs of approximately 4 h were made at temperatures of 280, 300 and 320 K. With PG002 analyzers, the measured energy resolution was 17.5 μeV FWHM and the energy transfer window was ±

400 μeV, giving a dynamic range of 2 - 75 ps. The MODES suite of programs was used to derive the scattering functions $S(Q,E)$.[27]

Following our previous work,[18,19,20,21] the resolution-corrected scattering functions were fitted by the expression:

$$S(Q,E) = c_1(Q)\,\mathrm{L}(W_1,E) + c_2(Q)\,\mathrm{L}(W_2,E) + a + bE \tag{1}$$

where $\mathcal{L}(W_n, E)$ denotes a Lorentzian function with unit area and a FWHM of W_n, and the linear background terms allow for a slowly varying inelastic scattering component. The Q dependence of W_n was least-squares-fitted by the following expressions:

$$W_1 = \frac{\alpha_1 + \beta_1 Q^2}{(1+\gamma_1 Q^2)}, \tag{2a}$$

$$W_2 = \alpha_2 + \beta_2 Q^2. \tag{2b}$$

In the spirit of the TBCD model,[28] the parameters α_i and β_i have the following significance:

$$\beta_1 = 2\hbar D, \tag{3a}$$

$$\gamma_1 = \frac{l^2}{6}, \tag{3b}$$

where D is the translational diffusion constant and l an effective jump distance, and

$$\alpha_2 = \frac{2\hbar}{3\tau_R}, \tag{3c}$$

where τ_R is a relaxation time for orientational diffusion, while β_2 has two compensating components, one identified with $2\hbar D$ and the other reflecting the increasing contribution of higher-order rotational terms as Q increases. The constant α_1 in Eq. (2a) is zero in the TBCD model but we allow it to take small non-zero values to allow for small differences between the true resolution function and the vanadium standard and, in the case of the d-fruc+H_2O measurements, a possible contribution from the slower dynamics of the sugar molecules.

III. Results and discussion

A. MD Simulations

Water and sugar self-diffusion coefficients, D_{water} and $D_{glucose}$, were obtained from the mean-square displacements as a function of time by using the Debye-Einstein relation.[29] The diffusion constants of water obtained at the different concentrations are compared with

previous NMR and QENS data in Fig. 2. The most obvious result is a strong reduction in the diffusion rate as the glucose concentration is increased. The MD results are considerably closer to the QENS values of Talón *et al.*[18] and to the ^{2}H NMR results of Moran *et al.*[30] than the earlier MD simulations of Roberts *et al.*[31] There are two probable reasons for this difference. First, the SPC/E model for water used in this study is known to give a more realistic diffusion coefficient ($2.49 \pm 0.05.10^5$ cm^2s^{-1}) than the SPC model used by Sonoda *et al.*[32], which gives a value a factor ~ 1.5 too high.[33] Secondly, while in the present study the values for the densities used in the simulations are taken from the experimental data in the literature,[34,35,36] Roberts *et al.*[31] used values for the concentrated solutions somewhat higher.

Concentration and temperature dependence—The temperature and concentration dependence of the diffusion constants of water and sugar are shown in Fig. 3 and 4, respectively. It can be seen that there is good agreement between the numerical and experimental values.[18,19] (Fig. 3b and 4b) The numerical value for D_{water} at 280 K decreases by a factor of 1.6 between 1 and 3 molal, reasonably consistent with the experimental factor of 2.2.[18] This factor remains almost constant (1.4-1.6) over the entire temperature range investigated, indicating that the activation energy is almost constant between 1 and 3 molal, a trend also observed in the QENS[18] and dielectric spectroscopy measurements.[37] However, the absolute values remain higher than the experimental ones, which could be slightly underestimated since a low percentage of the total scattering comes from the solute. On the other hand, the simulation value of $D_{glucose}$ at 280 K decreases by a factor of ~2.5 between 1 and 3 molal and by a factor of ~5.5 between 1 and 5 molal, consistent with the experimental values of ~2.1 and ~5.6.[19] Nevertheless, the simulations reproduce the general trends for both solvent and solute molecules. The change in the dynamical regime of both types of molecules around 3 molal (Figs. 3 and 4) corresponds to the appearance of solute-solute interactions, as observed by near infrared spectroscopy (NIR),[38] by QENS on fructose solutions,[39] and in the earlier simulations of glucose solutions.[31] The solvation of glucose molecules leads to a disruption of the local water hydrogen bond (H-bond) network by a steric effect in favor of new H bonds between the sugar and water molecules. The solute has a very localized influence on the water H-bond network, as shown by the relatively small decrease in D_{water} between 0 and 1 molal. Around 3 molal,[38] the appearance of sugar-sugar H bonds leads to the formation of localized sugar clusters, considerably modifying the water H-bond network. When the sugar concentration is further increased, the decrease in the number of water-water H bonds in favor of both sugar-water and sugar-sugar H bonds leads to a drastic change in the behavior of the water molecules, particularly a general slowing down of the translational dynamics, as observed in NMR,[30] QENS,[18] and NIR measurements[38] and in MD simulations.[40,41]

Concentration-temperature analogy—An especially interesting feature is the equivalence of different solutions from a dynamical point of view in the concentration/temperature diagram. The Fig. 5 highlights some similarities found in the translational diffusion coefficients of both glucose and water molecules obtained from the simulations. It appears that an increase in the glucose concentration is equivalent to a decrease in temperature. For example, if we consider a 3 molal sugar solution at 280 K, we find that a decrease in temperature by 20 K or an increase in concentration by 2 molal has the same effect for both solute and solvent molecules. An analogy has been made between the effects of certain solutes on the local structure of the water and those of temperature or pressure on the connectivity of the water network: D-glucose in dilute system is equivalent to a decrease in temperature, *i.e.* to an increase of the ordering. Talón *et al.* (QENS),[18] Giangiacomo (NIR),[38] and Paolantoni *et al.* (Raman)[42] found similar analogies that support this interpretation. This trend has been observed experimentally for both monosaccharide[14] and disaccharide solutions.[43] At higher temperatures, above 320 K, the temperature/concentration analogy seems to break down, consistent with the known decrease with temperature of hydrogen bonding in pure liquid water,

so that it seems to be valid only in a restricted window of the concentration/temperature diagram.

B. QENS Experiments

Fits of Eq. (2) to the IRIS measurements on the H_2O and d-fruc+H_2O samples are shown in Fig. 6, and those for h-fruc+D_2O on the Fig.7. The values derived for D, l and τ_R from Eq. (3) for the dynamics of the solvent and solute molecules are given in Table 3.

Dynamics of pure water—The activation energy for translational diffusion of pure water obtained from the temperature dependence is 4.0 ± 0.4 kcal.mol^{-1}, similar to that obtained earlier for the 1:20 glucose solution (3.8 ± 0.4 kcal.mol^{-1}).[18] For comparison, Teixeira *et al.*[28] reported $D = 1.34\times10^{-5}$ cm^{2}s^{-1} and an activation energy of 3.6 kcal.mol^{-1}, in good agreement with our values.

Dynamics of monosaccharide molecules in solution—The value of D_{fructose} in a 2.3 molal solution is similar to that of β-furanose (0.095×10^{-5} cm^{2}s^{-1}) and β-pyranose (0.092×10^{-5} cm^{2}s^{-1}), measured at 277 K by PFG-NMR.[14] Our value, $D_{\text{fructose}} = 0.14\times10^{-5}$ cm^{2}s^{-1}, has the same order of magnitude as that observed for glucose[19] but is slightly higher. This behavior can be explained by (1) the remarkably low viscosity value of fructose solutions compared with other monosaccharides,[44,45] (2) the difference in the number of tautomers (2 for the glucose *vs.* 4 for the fructose – *cf.* Fig. 1)[13,32], and (3) the slightly higher hydrophobicity of the fructose, especially in the β-D-fructopyranose form in which two hydrogens atoms are bonded on the C1 carbon.[45] Thus, the fructose tends to disrupt the H-bond network of the water more than the glucose. The orientational relaxation time of fructose, τ_R = 3.4 ps, is almost constant over the whole temperature range investigated, implying a very low activation energy.

Dynamics of water molecules in solution—The values of D_{water} extracted from the IRIS measurement are compared in Fig. 8 with earlier experimental and numerical results.[14,28,31,32,39,45] Both sets are in good agreement with the ^{1}H NMR results of Mahawanich *et al.*[45] but slightly lower than those measured by QENS by Feeney *et al.*[39] and by NMR by Rampp *et al.*[14] on solutions of fully protonated fructose in water. Nevertheless, the global trend of the concentration dependence is similar in the two cases. The earlier simulations[31,32] are not in good agreement with the experimental results except for the lower concentration studied by Roberts *et al.*[31].

At 280 K and 2.3 molal, the values of D_{water} measured in the fructose solution is 40% lower than in the corresponding glucose solution,[18] while the orientational relaxation time τ_R of water, 4.3 ps, is longer than in glucose (τ_R = 1.4 ps). A similar reduction (~ 50%) is obtained when we compare with the numerical values that we calculate. Water molecules are then less mobile in fructose solutions as indicated by the lower values of D_{water} and the relatively small jump distance l, showing that the solvent molecules are more localized in the fructose solutions than in the glucose. It gives then an indication of the extent of the H-bonds occurring in these two monosaccharide solutions.

IV. Conclusions

In contrast to previous simulations,[31,32] the results of MD simulations on glucose solutions are in excellent agreement with experimental results[18,19,30] over the whole range of sugar concentrations studied. They indicate a dynamical analogy between higher solute concentrations and lower temperatures. The dehydration process thus leads to a physico-chemical state equivalent to higher temperature. While this hypothesis seems to be validated by the few experimental results in the literature, a complete systematic study over a wide range

of concentration and temperature for several mono- and disaccharides is needed. If confirmed, this concentration-temperature analogy could provide a key explanation of the bioprotective phenomena observed in many living organisms.[3,4,46]

The experimental results on fructose solutions show a qualitative similarity in behavior with the glucose solutions. First, the dynamics of the water molecules are almost the same, showing that for these relatively low concentrations the different topologies and molecular sizes of two monosaccharides do not make a significant difference in the dynamical properties of the water molecules. However, the translational diffusion of the fructose molecules is slightly faster than that of the glucose.

Acknowledgments

GL is indebted to the Region Centre for a SOLEIL scholarship. This work was supported by grant GM63018 from the US National Institutes of Health in US, and the Centre National de la Recherche Scientifique in France. The authors acknowledge the support of the CCLRC in providing the neutron research facilities for this work. Experiments at the ISIS Pulsed Neutron and Muon Source were supported by a beamtime allocation from the Science and Technology Facilities Council.

References

1. Chenlo F, Moreira R, Fernández-Herrero C, Vázquez G. J Food Eng 2006;74:324.
2. Rodrigues S, Fernandes FAN. J Food Eng 2007;80:678.
3. Watanabe M. Appl Entomol Zool 2006;41(1):15.
4. Wolfe J, Bryant G. Cryobiology 1999;39:103. [PubMed: 10529304]
5. Kasuga J, Arakawa K, Fujikawa S. New Phytologist 2007;174:569. [PubMed: 17447912]
6. Dashnau JL, Vanderkooi JM. J Food Sci 2007;72(1):R1.
7. Chiantia S, Kahya N, Schwille P. Langmuir 2005;21:6317. [PubMed: 15982037]
8. Eisenberg, D.; Kauzmann, W. The Structure and Properties of Water. Oxford University Press; Oxford: 1969.
9. Stillinger FH. Science 1980;209:451. [PubMed: 17831355]
10. Ueda K, Brady JW. Biopolymers 1996;38(4):461. [PubMed: 8867209]
11. Naidoo KJ, Brady JW. J Am Chem Soc 1999;121(10):2244.
12. Gharsallaoui A, Rogé B, Génotelle J, Mathlouthi M. Food Chem 2008;106:1443.
13. Fuchs K, Kaatze U. J Phys Chem B 2001;105:2036.
14. Rampp M, Buttersack C, Lüdermann HD. Carbohydrate Res 2000;328:561.
15. Gray MC, Converse AO, Wyman CE. Appl Biochem & Biotech 2003;105-108:179.
16. Cockman M, Kubler DG. J Carbohydrate Chem 1987;6(2):181.
17. Migliori M, Gabriele D, Di Sanzo R, de Cindio B, Correra S. J Chem Eng Data 2007;52:1347.
18. Talón C, Smith LJ, Brady JW, Lewis BA, Copley JRD, Price DL, Saboungi ML. J Phys Chem B 2004;108:5120.
19. Smith LJ, Price DL, Chowdhuri Z, Brady JW, Saboungi ML. J Chem Phys 2001;120:3527. [PubMed: 15268513]
20. Lelong G, Price DL, Douy A, Kline S, Brady JW, Saboungi ML. J Chem Phys 2005;122:164504. [PubMed: 15945690]
21. Lelong G, Price DL, Brady JW, Saboungi ML. J Chem Phys 2007;127:065102. [PubMed: 17705626]
22. Berendsen HJC, Grigera JR, Straastsma TP. J Phys Chem 1987;91:6269.
23. Neria E, Fischer S, Karplus M. J Chem Phys 1996;105(5):1902.
24. Brooks BR, Bruccoleri RE, Olafson BD, Swaminathan S, Karplus MJ. J Comput Chem 1983;4:187.
25. van Gunsteren WF, Berendsen HJC. Mol Phys 1977;34:1311.
26. Adams, MA.; Howells, WS.; Telling, MTH. Rutherford-Appleton Laboratory Technical Report RAL-TR-2001-002. 2001.

27. Telling, MTH.; Howells, WS. MODES Manual. ISIS Facility Rutherford-Appleton Laboratory; 2003. unpublished
28. Teixeira J, Bellissent-Funel MC, Chen SH, Dianoux AJ. Phys Rev A 1985;31:1913. [PubMed: 9895699]
29. Allen, MP.; Tildesley, DJ. Computer Simulation of Liquids. Vol. Chapter 2. Oxford Science Publications; 1989.
30. Moran GR, Jeffrey KR, Thomas JM, Stevens JR. Carbohydrate Res 2000;328:573.
31. Roberts CJ, Debenedetti PG. J Phys Chem B 1999;103:7308.
32. Sonoda MT, Skaf MS. J Phys Chem B 2007;111:11948. [PubMed: 17887790]
33. Mahoney MW, Jorgensen WL. J Chem Phys 2001;114(1):363.
34. Comesaña JF, Otero JJ, García E, Correa A. J Chem Eng Data 2003;48:362.
35. Cerdeiriña CA, Carballo E, Tovar CA, Romaní L. J Chem Eng Data 1997;42:124.
36. Ji P, Fei W, Tan T. J Chem Eng Data 2007;52:135.
37. Jansson H, Bergman R, Swenson J. J Non-Cryst Solids 2005;351:2858.
38. Giangiacomo R. Food Chem 2006;96:371.
39. Feeney M, Brown C, Tsai A, Neumann D, Debenedetti PB. J Phys Chem B 2001;105:7799.
40. Molinero V, Çagin T, Goddard WA III. Chem Phys Lett 2003;377:469.
41. Lee SL, Debenedetti PG, Errington JR. J Chem Phys 2005;122:204511. [PubMed: 15945756]
42. Paolantoni M, Sassi P, Moressi A, Santini S. J Chem Phys 2007;127:024504. [PubMed: 17640134]
43. Affouard F, Bordat P, Descamps M, Lerbret A, Magazù S, Migliardo F, Ramirez-Cuesta AJ, Telling MFT. Chem Phys 2005;317:258.
44. Mathlouthi M, Seuvre AM. J Chem Soc, Faraday Trans I 1988;84(8):2641.
45. Mahawanich T, Schmidt SJ. Food Chem 2004;84:169.
46. Scott P. Annals of Botany 2000;85:159.

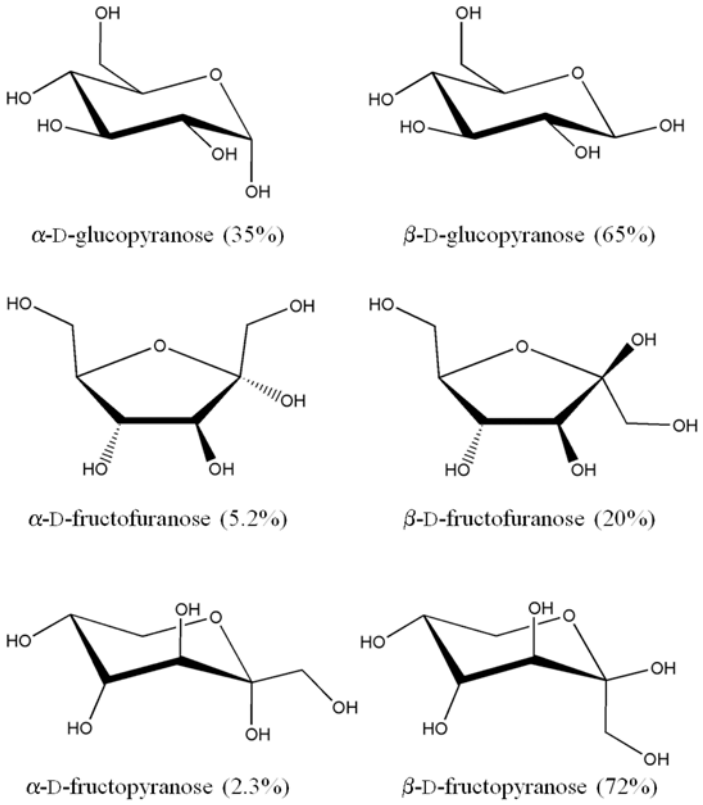

Fig. 1.

Stick representation of the different tautomers of D-glucose and D-fructose. The percentage values correspond to the relative abundance of each isomer at the tautomeric equilibrium.[13, 14]

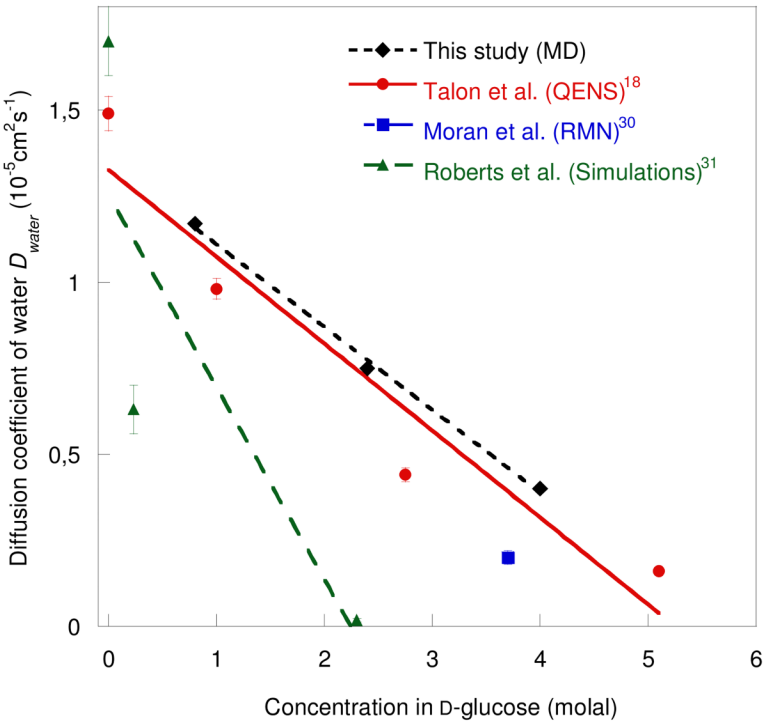

Fig. 2.

Diffusion coefficient of water molecules in glucose solutions at 280K obtained in this study, together with experimental and simulation values results in the literature.[18,30,31] The solid lines represent linear fits.

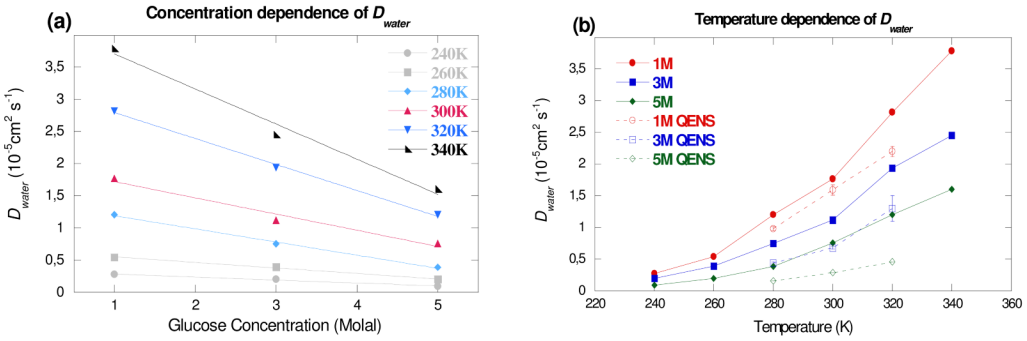

Fig. 3.

Water diffusion constant in glucose solutions from MD simulations (a) as a function of glucose concentration and (b) as a function of temperature. The QENS values shown are extracted from the work of Talón et al.[18] The solid lines in Fig. 3(a) represent linear fits whereas those in Fig. 3(b) are a guide for the eyes.

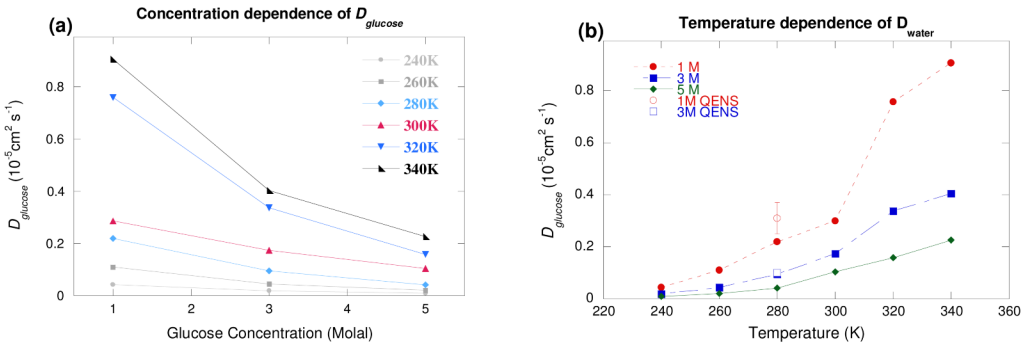

Fig. 4.

Glucose diffusion constant from MD simulations (a) as a function of concentration and (b) as a function of temperature. The QENS experimental values shown in Fig. 4(b) are extracted from this work. The solid lines are a guide for the eyes.

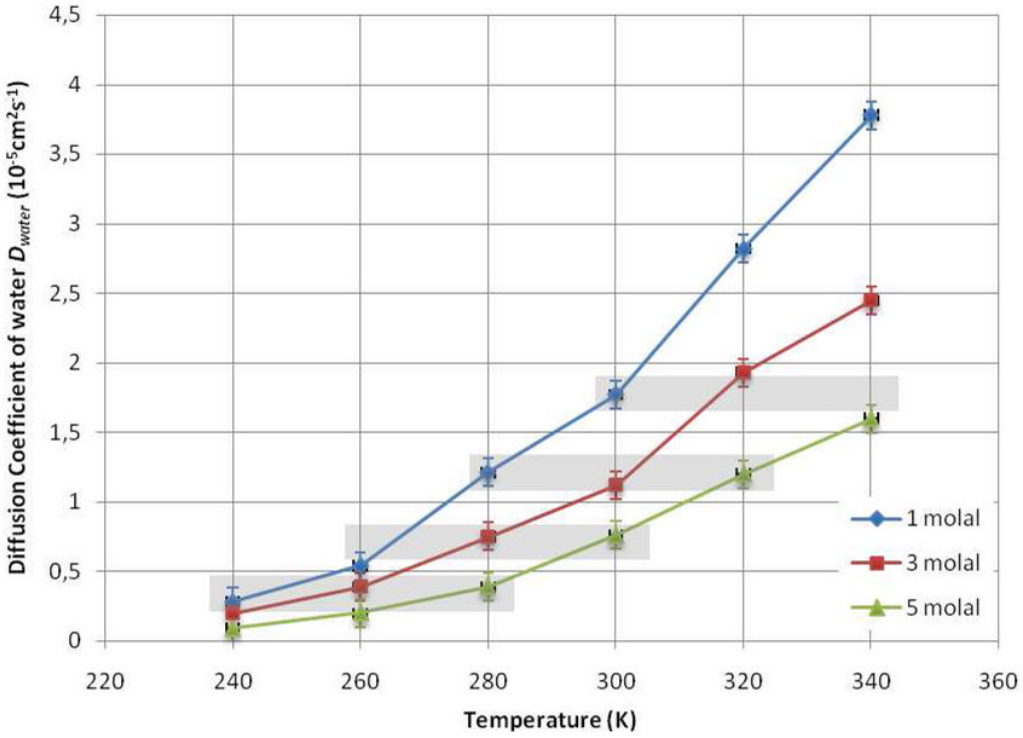

Fig. 5.

Evolution of the MD diffusion constants obtained from the MD simulations for solutions of 1, 3 and 5 molal. The grey rectangles show the dynamical analogies existing between the different solutions in the composition / temperature diagram.

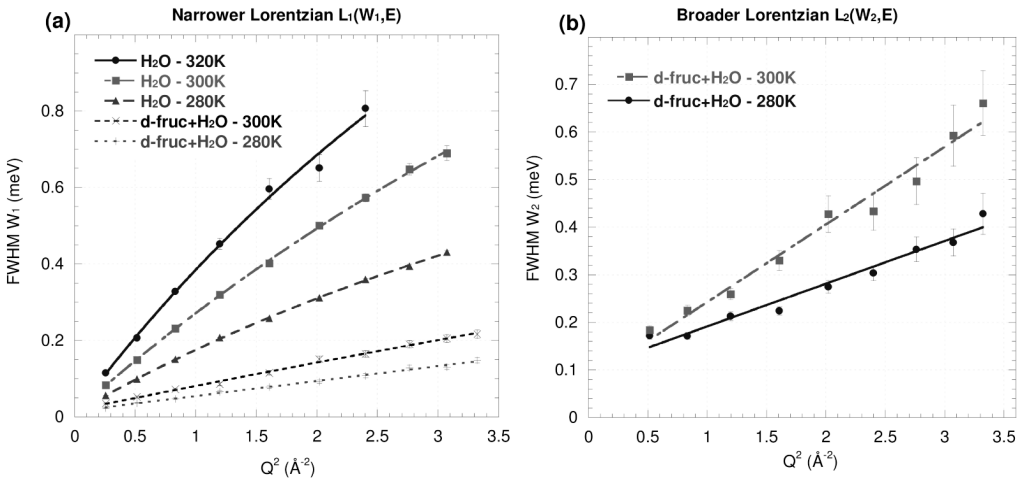

Fig. 6.

FWHM of (a) the narrower Lorentzian W_1 and (b) the broader Lorentzian W_2 fitted to the QENS spectra at different values of Q for the water and d-fruc+H_2O at 280, 300 and 320K. The lines represent fits of Eq. (2).

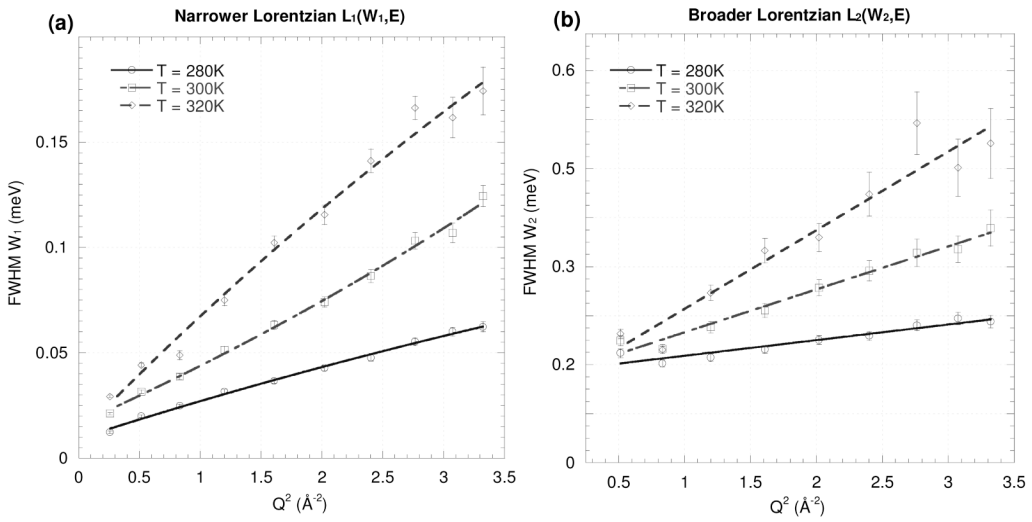

Fig. 7.

FWHM of the narrower Lorentzian W_1 (a) and of the broader Lorentzian W_2 (b) fitted to the QENS spectra at different values of Q for the h-fruc+D_2O sample measured at 280, 300 and 320K. The lines represent fits of Eq. (2).

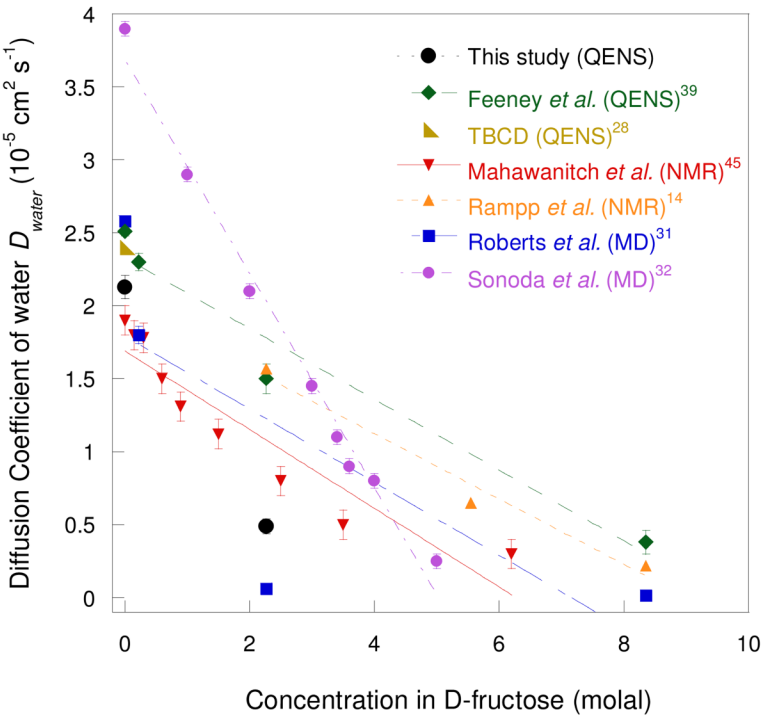

Fig. 8.
Diffusion coefficient of water molecules in fructose solutions at 300K obtained in this study, together with experimental and simulation results in the literature.

Table 1

Summary of the solutions and parameters used in the simulations

Molality	# glucose	# water	density	number density	box size
			g/cm^3	at./Å^3	Å
1 molal	18 (6α, 12β)	995	1.0615	0.1032	32.1527
3 molal	36 (12α, 24β)	667	1.1433	0.1066	29.9447
5 molal	60 (20α, 40β)	666	1.2063	0.1095	31.5474

Table 2

Characteristics of the different solutions

#	Name	Solution	Concentration			Probed Dynamics
			wt. %	sugar:water	molality	
1	**H_2O**	H_2O	0%	-	-	Water
2	**d-fruc+H_2O**	Fructose:H_2O	29%	**1 $C_6H_5D_7O_6$: 24.5**	2.3 molal	Solvent
3	**h-fruc+D_2O**	Fructose:D_2O	29%	**1 $C_6D_5H_7O_6$: 24.5**	2.3 molal	Solute

Table 3

Diffusion constants of the water molecules D_{water} (H_2O and d-fruc+H_2O) and of the fructose molecules $D_{fructose}$ (h-fruc+D_2O), effective jump distance l and relaxation time for orientational diffusion τ_R calculated from the fits of Eq. (3). These results (bold) are compared to previous ones (italic) obtained for glucose solutions at 280 K.[18,19] (Water dynamics: d-gluc+ H_2O / Solute dynamics: h-gluc+ D_2O)

	Sample	Temperature (K)	D (10^{-5} cm^2 s^{-1})	l (Å)	τ_R (ps)
This work	**H_2O**	280	1.4 ± 0.04	0.81 ± 0.01	-
		300	2.13 ± 0.08	0.73 ± 0.04	-
		320	3.3 ± 0.6	0.9 ± 0.3	-
	d-fruc+H_2O, 1:24.5	280	0.3 ± 0.04	0.2 ± 0.5	4.3 ± 0.4
		300	0.49 ± 0.05	0.4 ± 0.3	4.2 ± 0.8
	h-fruc+D_2O, 1:24.5	280	0.14 ± 0.01	0.5 ± 0.2	3.2 ± 0.1
		300	0.24 ± 0.02	0.4 ± 0.3	3.4 ± 0.2
		320	0.45 ± 0.08	0.6 ± 0.3	3.2 ± 0.4
*Talon et al.*18	*d-gluc+H_2O, 1:55*	*280*	*0.98 ± 0.03*	-	-
	d-gluc+H_2O, 1:20	*280*	*0.44 ± 0.02*	-	-
*Smith et al.*19	*h-gluc+D_2O, 1:55*	*280*	*0.252 ± 0.002*	*0.2*	-
	h-gluc+D_2O, 1:20	*280*	*0.123 ± 0.002*	*1.4*	-